LIGHTWEIGHT STRUCTURES in CIVIL ENGINEERING
CONTEMPORARY PROBLEMS
Monograph from Scientific Seminar
Organized by Polish Chapters of
International Association for Shell and Spatial Structures
Lodz University of Technology
Faculty of Civil Engineering, Architecture and Environmental Engineering
XXIV LSCE
Łódź, 7th of December 2018 (Friday)

ROTATIONAL RESTRAINT PROVIDED TO COLD-FORMED Z-PURLINS BY TRAPEZOIDAL SHEETING IN NEGATIVE POSITION

M. Gajdzicki [1)]
[1)] PhD, Faculty of Civil Engineering, Architecture and Environmental Engineering, Lodz University of Technology, POLAND, *michal.gajdzicki@p.lodz.pl*

ABSTRACT: The method of fastening the trapezoidal sheeting to the supporting beams has a significant influence on their rotational restraint, and thus their buckling resistance. Commonly one fastener is placed in each trough of the sheeting. In this paper the arrangement of two fasteners located near the trapezoidal sheeting webs in every second trough was investigated. Such an arrangement, with the same number of fasteners along the purlin, increases the value of the rotational stiffness C_D, which was confirmed in 28 experimental tests and corresponding numerical simulations in the Abaqus software. The numerical investigation was also extended to the additional 8 models, which had not been tested experimentally. Based on the results from the numerical analysis, same changes were proposed in the current provisions of Eurocode 3-1-3 regarding the rotational coefficient C_{100}, but also the new rules for cases not covered by the provisions of this code were presented.

Keywords: cold-formed Z-purlin, rotational restraint, sheet-to-purlin fastener, rotational spring stiffness.

1. INTRODUCTION

Cold-formed steel purlins support a roof cladding formed from profiled steel sheeting. Trapezoidal sheets, interconnected with each other, create with these beams a plate-shell-bar system, that imposes restraints on the attached beams. The nature of this restraints results from the method of fixing the sheeting to the beams and the characteristics of the connected parts of the structural system. These restraints are imposed mostly on the beam top flange, rarely on both. In practice, the beam sections are connected to the trapezoidal sheets, so densely that this restraint is considered to be continuous. The linear joint between the trapezoidal sheeting and the purlin provides lateral and rotational restraints to the top flange of the attached purlin (Fig 1). Due to significant shear stiffness of the sheeting, the lateral restraint is assumed to be full ($K_y = \infty$) for cold-formed purlins. In contrast, the rotational one is always partial and characterized by the rotational spring stiffness C_D given by:

$$C_D = 1/(1/C_{D,A} + 1/C_{D,C}) \quad (1)$$

where: $C_{D,A}$ is the rotational stiffness of the connection between the purlin and the sheeting; $C_{D,C}$ is the rotational stiffness corresponding to the flexural stiffness of the sheeting.

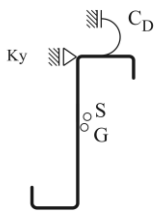

Fig.1 Boundary conditions of Z- purlin according to [1]

If the rotational stiffness corresponding to the flexural stiffness of the sheeting $C_{D,C}$ is assumed infinite, the total rotational stiffness C_D depends only on the rotational stiffness of the connection between the sheeting and the purlin $C_{D,A}$. Provided that the sheet-to-purlin fasteners are positioned centrally on the top flange of the purlin and that there is no thermal insulation layer between the purlins and the sheeting, the value of $C_{D,A}$ for trapezoidal sheeting connected to the top flange of the purlin may be determined as follows:

$$C_{D,A} = C_{100}\, k_{ba}\, k_t\, k_{bR}\, k_A\, k_{bT} \quad (2)$$

where: C_{100} is a rotation coefficient, representing the value of C_D, when the flange width is equal to 100 mm, given in Table 10.3 in Ref 1; k_i are the numerical coefficients that depend on the width of the flange, trapezoidal sheeting geometry; sheeting arrangement; the spacing of fasteners; the values and direction of the load transferred from the sheeting to the purlin.

The formulae for coefficients k_i can also be found in Eurocode 3-1-3. However there are many limitations on the use of Eqn (2). The C_{100} values are given only for washer diameters equal 22 mm for gravity loading and 16 mm for uplift loading. The sheet fasteners must have the diameters of 6.3 mm and the steel washer must have a thickness more than 1 mm. In Ref 2 it has been proved that some of these limitations may be ignored, as the rotational stiffness values do not differ significantly despite the use of fasteners with different parameters than those defined in Ref 1.

In the design situations, in which the geometric limitations specified in Ref 1 are not satisfied, the C_D value cannot be estimated from simple formulas and should be calculated from Eqn (4). This requires the value of the lateral spring stiffness K given to the free flange of the purlin by the sheeting, determined by testing. Annex A of the Eurocode 3-1-3 describes the procedure for the experimental determination of the stiffness K (Eqn (3)) and recommends two test set-ups with different static schemes: the cantilever and the beam scheme. The first experimental tests to specify the design provisions for determining the value of the rotational stiffness C_D were conducted by Lindner in 1986-98 – Refs 3, 4. Afterwards, the relevant equations were expanded by

coefficients included in Eqn (2) depending on the sheet-to-purlin connection properties, proposed by Höglund, Vrany and Lindner – Ref 5.
In above tests, the measured linear displacement δ of upper flange in the direction of the force F depends on the flexibility of two types: the connection between the purlin and the sheeting ($1/K_A$) and distortion of the purlin cross-section ($1/K_B$). The value of the force F in Eqn (3) is the load per unit length of the test specimen that produces a lateral deflection of $\delta = h/10$ where h is the height of the purlin cross-section.

$$1/K = (1/K_A + 1/K_B) = \delta/F \quad (3)$$

According to Ref 1, if the total lateral spring stiffness K per unit length is obtained by testing, the value of the total rotational spring stiffness C_D for gravity and uplift loading should be determined from:

$$C_D = h^2 / (1/K - 1/K_B) = K_A h^2 \quad (4)$$

Although the test set-up is not of significant size, such experimental studies are always expensive and time-consuming. Therefore, researchers propose advanced numerical models to predict the behaviour of purlin-sheeting system or to simulate standard test to determine the C_D value. In Refs 6 and 7 authors initially presented the full, and later the simplified finite element models to study the interactional behaviour of the purlin-sheeting system and its effect on the load-carrying capacity. The extensive parametric studies using advanced finite element models were the subject of investigation presented in Ref 8, where the authors included the contact modelling and hyperelastic behaviour of neoprene washers. The numerical model which consists of the sheeting, the Z-purlin section, the fastener and the washers was described in Refs 9 and 2. As all elements of the investigated system were modelled the interaction occurred between the parts of the model and distortion of the profile cross-section was taken into account. Such a detailed modeling of the contact zone in Ref 2 allowed for a thorough numerical analysis of the impact of the fastener parameters on the final value of the C_D stiffness.

2. THE AIM OF THE STUDY

The primary aim of the research herein was to investigate the influence of the sheet-to-purlin fasteners arrangement on the value of the C_D stiffness. Currently, it is recommended that the sheeting should be fastened using self-tapping screws in every or in every second trough of the trapezoidal sheeting (arrangement 1+1) - Fig 2a. In this study, the case where two fasteners were located near the trapezoidal sheeting webs in every second trough (arrangement 2+0) was analyzed - Fig 2b. The load applied to the free flange of profile is transferred to the sheet by the fasteners, which are always in tension due to the lever effect in the connection. The bending stiffness of the trough panel is small. Therefore, it is reasonable to locate the fasteners near the sheet webs. That significantly reduces the deformation of the connection, which consequently increases the value of lateral stiffness K_A and the C_D stiffness.

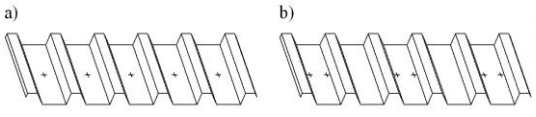

Fig.2 The Arrangement of the sheet-to-purlin fasteners:
a) 1+1, b) 2+0

In order to investigate the influence of sheet-to-purlin fastener arrangement on the value of the rotational stiffness C_D, 24 test specimens were built varying with the following parameters:
- geometry of trapezoidal sheet (T45x0.5; T55x0.5) – see Fig 5,
- width of the purlin flange connected to the sheet (48; 53; 60 or 68 mm) – see Fig 4,
- fastener arrangement (1+1; 2+0) - see Fig 2,
- load direction (U - uplift; G - gravity).

Due to the difficulty in obtaining complete fixing of the trapezoidal sheet in the cantilever scheme, the tests described in this paper were carried out using the beam scheme (Fig 3) recommended by Ref 1.

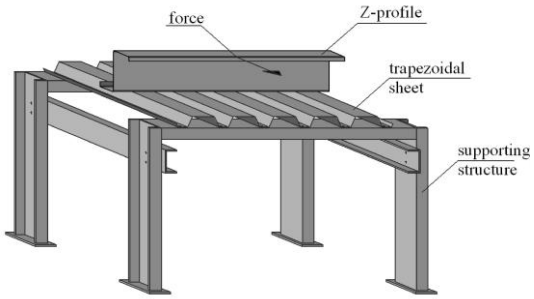

Fig.3 The scheme of the used test set-up

The numerical simulations using advanced FEA models included not only the specimens tested experimentally, but were also extended with additional 8 models to obtain numerical results for all possible combinations of the trapezoidal sheeting trough width and the upper purlin flange being in contact. The specification of all 32 specimens is presented in Table 1 (for those marked with an asterisk, only the numerical results were obtained). In the specimen symbol, numbers in brackets denotes the width and the length of the contact zone between the trapezoidal trough and the upper purlin flange.

Table 1. Test specimen

No.	Sheeting	Purlin	Fastener	Load
1.	T45x0.5(95.5)	Z200x1.5(53)	1+1	G
2.	T45x0.5(95.5)	Z200x1.5(53)	2+0	G
3.	T45x0.5(95.5)	Z200x1.5(48)	1+1	G
4.	T45x0.5(95.5)	Z200x1.5(48)	2+0	G
5.*	T45x0.5(95.5)	Z200x1.5(68)	1+1	G
6.*	T45x0.5(95.5)	Z200x1.5(68)	2+0	G
7.*	T45x0.5(95.5)	Z200x1.5(60)	1+1	G
8.*	T45x0.5(95.5)	Z200x1.5(60)	2+0	G
9.	T55x0.5(136.5)	Z200x1.5(68)	1+1	G
10.	T55x0.5(136.5)	Z200x1.5(68)	2+0	G
11.	T55x0.5(136.5)	Z200x1.5(60)	1+1	G
12.	T55x0.5(136.5)	Z200x1.5(60)	2+0	G
13.	T55x0.5(136.5)	Z200x1.5(53)	1+1	G
14.	T55x0.5(136.5)	Z200x1.5(53)	2+0	G
15.	T55x0.5(136.5)	Z200x1.5(48)	1+1	G
16.	T55x0.5(136.5)	Z200x1.5(48)	2+0	G
17.	T45x0.5(95.5)	Z200x1.5(53)	1+1	U
18.	T45x0.5(95.5)	Z200x1.5(53)	2+0	U
19.	T45x0.5(95.5)	Z200x1.5(48)	1+1	U
20.	T45x0.5(95.5)	Z200x1.5(48)	2+0	U
21.*	T45x0.5(95.5)	Z200x1.5(68)	1+1	U
22.*	T45x0.5(95.5)	Z200x1.5(68)	2+0	U
23.*	T45x0.5(95.5)	Z200x1.5(60)	1+1	U
24.*	T45x0.5(95.5)	Z200x1.5(60)	2+0	U
25.	T55x0.5(136.5)	Z200x1.5(68)	1+1	U
26.	T55x0.5(136.5)	Z200x1.5(68)	2+0	U
27.	T55x0.5(136.5)	Z200x1.5(60)	1+1	U
28.	T55x0.5(136.5)	Z200x1.5(60)	2+0	U
29.	T55x0.5(136.5)	Z200x1.5(53)	1+1	U
30.	T55x0.5(136.5)	Z200x1.5(53)	2+0	U
31.	T55x0.5(136.5)	Z200x1.5(48)	1+1	U
32.	T55x0.5(136.5)	Z200x1.5(48)	2+0	U

The dimensions of the trapezoidal sheets and the Z-profile cross-sections, measured on the midlines, are shown in Figs 4 and 5. In all tests, the self-tapping fasteners with the diameter of 5.5 mm and the sealing washer with the diameter of 14 mm were used. In the specimen with the 1+1 arrangement, the fasteners were located in the center of the contact zone between the sheet trough and the purlin flange. In the tests with 2+0 arrangement, the fasteners were placed at the distance of 10 mm from the webs of trapezoidal sheet and in the half-width of purlin flange.

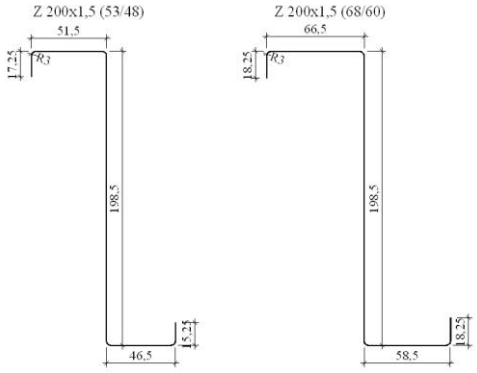

Fig.4 Geometry of Z-profiles

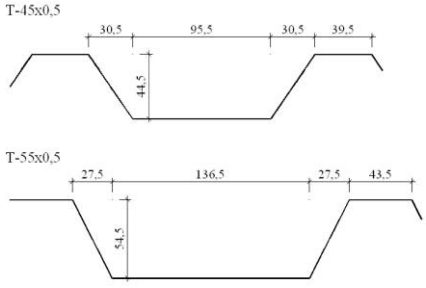

Fig.5 Geometry of trapezoidal sheet profiles

The values of rotational stiffness C_D obtained experimentally were compared with those from the numerical models. Due to the high consistency of the results, numerical values were then compiled with the values obtained on the basis of Eurocode 3-1-3 – Eqn (2). Such a comparison, made it possible to suggest some corrections in the code provisions for the cases already described there, but also to propose new provisions (new rotation coefficient C_{100}) for:
- 1+1 fastener arrangement and the uplift loading,
- 2+0 fastener arrangement and both loading cases.

3. RESULTS

3.1. Experimental tests

In all tests, the purlin free flange was loaded with the use of gravity force by changing its direction from vertical to horizontal using a block mounted on a cantilever (Fig 6).

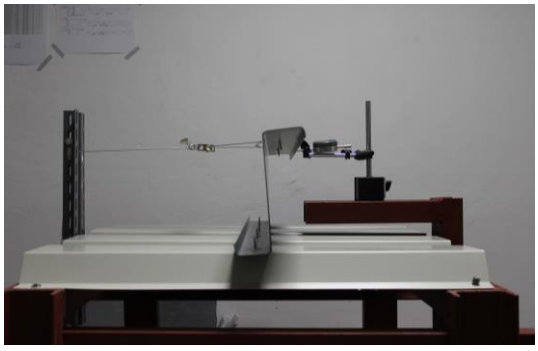
Fig.6 T55(136.5)-Z200(60)-11-G specimen

The load was applied in the increments of about 20 N/min. After each load increment linear displacement of the profile free flange was read from the digital linear displacement sensor. This allowed defining the load-displacement relationship (solid lines in Figs 8 and 9) and determining the value of the force F inducing displacement $\delta = h/10$.
The total lateral spring stiffness K per unit length was calculated substituting the obtained values of the force F and the displacement δ to Eqn (3). Afterwards, using Eqn (4) the value of rotational stiffness C_D was determined. The results obtained for the test specimens are shown in Table 2 for gravity loading and in Table 3 for uplift loading.

Table 2. Experimental results for gravity loading

No.	F [N]	K [N/mm]	K_B [N/mm]	K_A [N/mm]	C_D [Nm/m]	Ratio
1.	100.9	5.05	15.11	7.58	303	2.26
2.	160.7	8.03	15.11	17.16	686	
3.	74.0	3.70	15.63	4.85	194	2.37
4.	132.3	6.62	15.63	11.47	459	
9.	110.7	5.53	13.75	9.26	370	2.57
10.	174.4	8.72	13.75	23.84	954	
11.	98.4	4.92	14.44	7.46	298	1.70
12.	135.0	6.75	14.44	12.68	507	
13.	93.7	4.68	15.11	6.79	271	2.01
14.	143.4	7.17	15.11	13.65	546	
15.	66.6	3.33	15.63	4.23	169	1.47
16.	88.8	4.44	15.63	6.20	248	

Table 3. Experimental results for uplift loading

No.	F [N]	K [N/mm]	K_B [N/mm]	K_A [N/mm]	C_D [Nm/m]	Ratio
17.	115.1	5.75	20.32	8.03	321	2.11
18.	184.9	9.24	20.32	16.96	678	
19.	104.6	5.23	20.55	7.01	280	2.25
20.	178.3	8.92	20.55	15.75	630	
25.	122.3	6.11	19.66	8.87	355	1.98
26.	185.5	9.28	19.66	17.56	703	
27.	118.4	5.92	20.01	8.41	336	1.62
28.	162.0	8.10	20.01	13.61	544	
29.	92.6	4.63	20.32	6.00	240	1.65
30.	133.0	6.65	20.32	9.88	395	
31.	93.5	4.68	20.55	6.06	242	1.42
32.	121.5	6.07	20.55	8.62	345	

3.2. Numerical simulations

The non-linear FEA model shown in Fig 7 was developed to simulate the standard test and validated by experimental tests. The geometry of the finite element model was based on the midlines of Z- and sheet profiles. Each fastener between the trough of sheet and the attached profile flange were idealized by four connector elements (all six degrees of freedom constraint) spaced evenly around the hole with the diameter of 5.5mm.
The profile section and the trapezoidal sheet were discretized using the linear 4-node quadrilateral thick shell element S4R from the Abaqus finite element library. This element has six degrees of freedom per node utilizing the reduced integration. The element size of 5 mm by 5 mm was found to be appropriate for the trapezoidal sheet and the Z-profile section, based on the results of convergence study. Each of the surface pairs in contact was modelled using the master-slave surface pair option (Z-profile flange as master, sheet trough as slave). A classical elastic model of steel was used for all the FEA models, where the Young's

modulus and Poisson's ratio were assumed to be 210 GPa and 0.3, respectively.

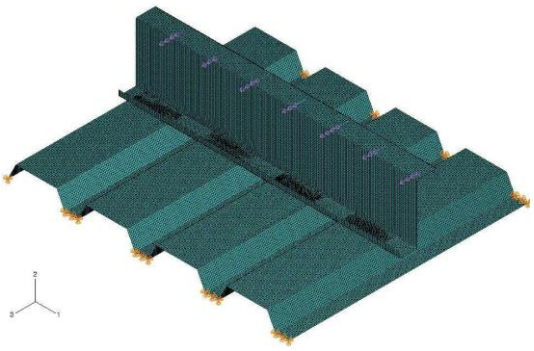

Fig.7 FEA model of T55(136.5)-Z200(60)-20-G specimen

The boundary conditions for the trapezoidal sheet were applied in such a way that three linear displacements were constrained at the end edge of each trough, with the rotation free. The load was applied as a uniform surface traction across the free flange of the profile section in the direction *3* in several increments (Fig 7), in order to obtain the displacement required in Eurocode 3-1-3. The load direction always remained parallel to the sheeting and independent from deformation. The two directions of loading was applied to reflect uplift and gravity loading.

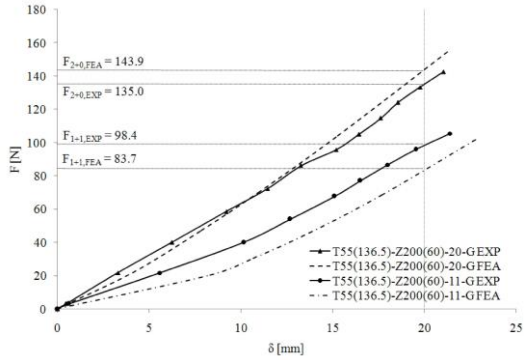

Fig.8 Load-displacement relationship for T55(136.5)-Z200(60) specimen – gravity loading

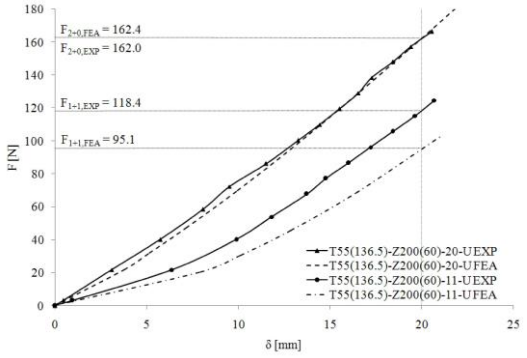

Fig.9 Load-displacement relationship for T55(136.5)-Z200(60) specimen – uplift loading

The values of the lateral displacement of free flange δ were collected after each increment of load for all models. This allowed creating the diagram of the relationship between load and displacement (dotted lines in Figs 8, 9) and to determine the load value corresponding to the required displacement equal to 1/10 the height of Z-profile. Next, the total spring stiffness applied to the free flange K (Eqn 3) and the value of the rotational spring stiffness C_D (Eqn 4) were calculated. Results from all 28 numerical models corresponding to the experimental tests and from 8 additional models are presented in Table 4 for gravity loading and in Table 5 for uplift loading.

Table 4. Numerical results for gravity loading

No.	F [N]	K [N/mm]	K_B [N/mm]	K_A [N/mm]	C_D [Nm/m]	Ratio
1.	100.5	5.02	15.11	7.53	301	3.08
2.	183.0	9.15	15.11	23.18	927	
3.	97.8	4.89	15.63	7.11	284	2.87
4.	177.0	8.85	15.63	20.40	816	
5.	120.6	6.03	13.75	10.75	430	3.20
6.	196.4	9.82	13.75	34.36	1374	
7.	112.4	5.62	14.44	9.20	368	2.92
8.	187.9	9.39	14.44	26.87	1075	
9.	90.4	4.52	13.75	6.74	270	2.46
10.	150.2	7.51	13.75	16.54	662	
11.	83.7	4.18	14.44	5.89	236	2.43
12.	143.9	7.20	14.44	14.34	574	
13.	75.5	3.77	15.11	5.03	201	2.44
14.	135.4	6.77	15.11	12.26	491	
15.	71.1	3.55	15.63	4.60	184	2.39
16.	128.9	6.45	15.63	10.97	439	

Table 5. Numerical results for uplift loading

No.	F [N]	K [N/mm]	K_B [N/mm]	K_A [N/mm]	C_D [Nm/m]	Ratio
17.	112.7	5.63	20.32	7.79	312	2.80
18.	210.3	10.52	20.32	21.80	872	
19.	107.8	5.39	20.55	7.31	292	2.61
20.	197.8	9.89	20.55	19.07	763	
21.	142.5	7.13	19.66	11.18	447	2.91
22.	245.1	12.25	19.66	32.51	1301	
23.	129.7	6.48	20.01	9.59	384	2.72
24.	226.6	11.33	20.01	26.12	1045	
25.	105.8	5.29	19.66	7.24	290	2.19
26.	175.7	8.78	19.66	15.88	635	
27.	95.1	4.75	20.01	6.24	249	2.19
28.	162.4	8.12	20.01	13.67	547	
29.	83,1	4.15	20.32	5.22	209	2.19
30.	146.2	7.31	20.32	11.41	456	
31.	77.7	3.88	20.55	4.79	192	2.08
32.	134.1	6.71	20.55	9.96	398	

From Table 4 and 5 it can be seen, that the 2+0 arrangement of the fasteners in the wide troughs of trapezoidal sheeting (in the negative position) gives twice to three times higher values of the C_D stiffness compared to the standard 1+1 arrangement. This difference does not depend on the width of the purlin flange, but it definitely increases for lower profile heights of trapezoidal sheets.

3.3. Comparison of experimental and numerical results

The comparison of load values F and calculated values of the C_D stiffness from the test results and the numerical ones are shown in Table 6 and 7. The ratios of the value obtained experimentally to that from numerical simulations are presented in columns 4 and 7. The value of that ratio for the applied force F for gravity loading varies from 0.69 to 1.31, but with the average of 1.01. Similar results were obtained for

uplift loadings, where the ratio values vary from 0.86 to 1.25, with average of 1.02. A slightly larger value spread of this ratio was obtained after calculating the values of the C_D stiffness, but still the average value was equal to 1.05 for gravity loading and 1.01 for uplift loading.

Table 6. Comparison of experimental and numerical results for gravity loading

No.	F_{EXP} [N]	F_{FEA} [N]	Ratio	$C_{D,EXP}$ [Nm/m]	$C_{D,FEA}$ [Nm/m]	Ratio
1.	100.9	100.5	1.00	303	301	1.01
2.	160.7	183.0	0.88	686	927	0.74
3.	74.0	97.8	0.76	194	284	0.68
4.	132.3	177.0	0.75	459	816	0.56
9.	110.7	90.4	1.22	370	270	1.37
10.	174.4	150.2	1.16	954	662	1.44
11.	98.4	83.7	1.18	298	236	1.27
12.	135.0	143.9	0.94	507	574	0.88
13.	93.7	75.5	1.24	271	201	1.35
14.	143.4	135.4	1.06	546	491	1.11
15.	66.6	71.1	0.94	169	184	0.92
16.	88.8	128.9	0.69	248	439	0.56

Table 7. Comparison of experimental and numerical results for uplift loading

No.	F_{EXP} [N]	F_{FEA} [N]	Ratio	$C_{D,EXP}$ [Nm/m]	$C_{D,FEA}$ [Nm/m]	Ratio
17.	115.1	112.7	1.02	321	312	1.03
18.	184.9	210.3	0.88	678	872	0.78
19.	104.5	107.8	0.97	280	292	0.96
20.	178.3	197.8	0.90	630	763	0.83
25.	122.3	105.8	1.16	355	290	1.23
26.	185.5	175.7	1.06	703	635	1.11
27.	118.4	95.1	1.25	336	249	1.35
28.	162.0	162.4	1.00	544	547	1.00
29.	92.6	83.1	1.11	240	209	1.15
30.	133.0	146.2	0.91	395	456	0.87
31.	93.5	77.7	1.20	242	192	1.26
32.	121.5	134.1	0.91	345	398	0.87

However, it should be noted that when the width of the profile flange increases, the values of force F obtained from numerical simulations change in a linear manner (dotted lines in Figs 10 and 11). That cannot be said about the values obtained from experimental tests (solid lines in Figs 10 and 11). This confirms the previous authors' conclusions, contained in Ref 2, that the standard test recommended in Eurocode 3-1-3 is very sensitive to a number of parameters that may strongly influence the rotational stiffness C_D (e.g. the position of the fastener on the width of the purlin flange).

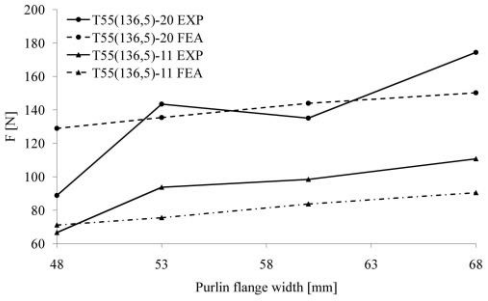

Fig.10 Relationship between force and purlin flange width for T55(136.5) specimens – gravity loading

From the initial numerical simulations, which will be the subject of further author's research, it turned out that in the case of T55(136.5)-Z200(60)-11-G model, where the fastener position was displaced by 5 mm from the midline of profile flange causes the change in the value of C_D stiffness by about 31%. It follows that for this model, the value of the force from the numerical simulations, would be the same as from the experiment when the fastener position was displaced about 4 mm towards the web of Z-profile, while for the model T55(136.5)-Z200(60)-20-G – less than 2 mm from the web.

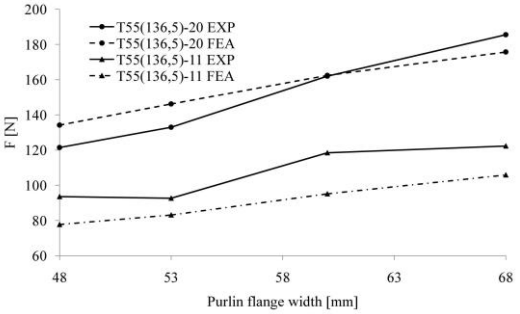

Fig.11 Relationship between force and purlin flange width for T55(136.5) specimens – uplift loading

Thus, despite the great care in assembling test specimens, imperfections could not be avoided, which caused that the results from experiments had greater dispersion of obtained values than those from numerical simulations. However, taking into account the average value for all models (1.01 for gravity loading and 1.02 for uplift loading), it can be concluded that the results from numerical simulations were in good agreement with experimental values. This confirms that the numerical model presented in the paper is a sufficiently accurate tool that can be used to conduct analyzes on the basis of which the design provisions for determining the value of C_D stiffness described in Ref 1 can be verified.

4. EUROCODE 3-1-3 PROVISIONS

For all 32 design situation tested in these research, the Eurocode 3-1-3 allows to determine the value of C_D stiffness (specify the values of rotation coefficient C_{100}) in only 8 of them (1+1 fastener arrangement under gravity loading). With the adopted geometry of the trapezoidal sheeting and the Z-section, the coefficients needed for Eqn (2) for the first test specimen assume the following values:

$$C_{D,100} = 3100 \text{ Nm/m} \quad (5)$$

$$k_{ba} = (b_a/100)^2 = (53/100)^2 = 0.281 \quad (6)$$

$$k_t = (t_{nom}/0.75)^{1.5} = (0.46/0.75)^{1.5} = 0.480 \quad (7)$$

$$k_{bR} = 185/b_R = 185/196 = 0.944 \quad (8)$$

$$k_A = 1.0 \quad (9)$$

$$k_{bT} = 1.0 \quad (10)$$

Thus, the value of C_D stiffness estimated on the basis of the Eurocode 3-1-3 is equal to:

$$C_D = 3100 \text{ x } 0.281 \text{ x } 0.480 \text{ x } 0.944 \text{ x } 1.0 \text{ x } 1.0 = 395 \text{ Nm/m} \quad (11)$$

The rotational stiffness values estimated in the analogous way for the remaining specimens under gravity loading and the fastener arrangement 1+1 are presented in Table 8 in column 3. From the comparison of results it can be concluded that under the current regulations, the Eurocode 3-1-3 overestimates the values of C_D stiffness (48% on average), which consequently leads to an overestimation of the load resistance of the Z-purlins restrained by the trapezoidal sheeting. It should be noted that the values of rotational coefficient C_{100} were determined based on the results of experimental tests performed in the 90s of the last century and as have already been shown in this paper and

in Ref 2, the test set-up used in the tests is very sensitive to a number of parameters and the results obtained at that time could have quite a big deviation. Therefore, in the column 5 the values of C_D stiffness determined from the same formulas are presented, but instead of C_{100} = 3100 Nm/m, a reduction of this coefficient to the value of 2100 Nm/m is proposed. Due to such a change, in the case of these 8 models, the ratio between the estimated stiffness values $C_{D,new}$ and the numerical simulation values is on average 1.0.

Table 8. Comparison of numerical results with Eurocode provisions (1+1 fastener arrangement under gravity loading)

No.	$C_{D,FEA}$ [Nm/m]	$C_{D,3\text{-}1\text{-}3}$ [Nm/m]	$C_{D,3\text{-}1\text{-}3}/C_{D,FEA}$	$C_{D,new}$ [Nm/m]	$C_{D,new}/C_{D,FEA}$
1.	301	395	1.31	267	0.89
3.	284	324	1.14	219	0.77
5.	430	650	1.51	440	1.02
7.	368	506	1.37	343	0.93
9.	270	508	1.89	344	1.28
11.	236	396	1.68	268	1.14
13.	201	309	1.54	209	1.04
15.	184	253	1.38	172	0.93
		Avg.	**1.48**	**Avg.**	**1.00**

In the remaining 24 cases for which the Eurocode 3-1-3 does not provide the value of the rotational coefficient C_{100}, its proposed values have been determined and are equal to:
- C_{100} = 5600 Nm/m – for 2+0 fastener arrangement under gravity loading (Table 9),
- C_{100} = 2300 Nm/m – for 1+1 fastener arrangement under uplift loading (Table 10),
- C_{100} = 5500 Nm/m – for 2+0 fastener arrangement under uplift loading (Table 11).

Table 9. Comparison of numerical results with proposed provisions (2+0 fastener arrangement under gravity loading)

No.	$C_{D,FEA}$ [Nm/m]	$C_{D,100}$ [Nm/m]	$C_{D,new}$ [Nm/m]	$C_{D,new}/C_{D,FEA}$
2.	927	5600	713	0.77
4.	816	5600	585	0.72
6.	1374	5600	1174	0.85
8.	1075	5600	914	0.85
10.	662	5600	918	1.39
12.	574	5600	715	1.25
14.	491	5600	558	1.14
16.	439	5600	457	1.04
			Avg.	**1.00**

Table 10. Comparison of numerical results with proposed provisions (1+1 fastener arrangement under uplift loading)

No.	$C_{D,FEA}$ [Nm/m]	$C_{D,100}$ [Nm/m]	$C_{D,new}$ [Nm/m]	$C_{D,new}/C_{D,FEA}$
17.	301	2300	293	0.94
19.	284	2300	240	0.82
21.	447	2300	377	0.84
23.	384	2300	294	0.77
25.	270	2300	377	1.30
27.	236	2300	294	1.18
29.	201	2300	229	1.10
31.	184	2300	188	0.98
			Avg.	**0.99**

Table 11. Comparison of numerical results with proposed provisions (2+0 fastener arrangement under uplift loading)

No.	$C_{D,FEA}$ [Nm/m]	$C_{D,100}$ [Nm/m]	$C_{D,new}$ [Nm/m]	$C_{D,new}/C_{D,FEA}$
18.	927	5500	700	0.80
20.	816	5500	575	0.75
22.	1301	5500	902	0.69
24.	1045	5500	702	0.67
26.	662	5500	902	1.42
28.	574	5500	702	1.28
30.	491	5500	548	1.20
32.	439	5500	449	1.13
			Avg.	**0.99**

In all of these cases, the average ratio between estimated stiffness values $C_{D,new}$ from the Eqn (2), taking into account the new value of the rotational coefficient C_{100}, and the values from the numerical simulations $C_{D,FEA}$, ranged around the value of 1.0.

5. CONCLUSIONS

It can be concluded that the 2+0 fastener arrangement, with the same number of fasteners along the length of the purlin, increases the values of rotational stiffness C_D. In the case of negative positioning of the trapezoidal sheeting, the ratio of C_D stiffness obtained for the 2+0 fastener arrangement to the 1+1 one for analyzed specimens varies from 2.08 to 3.20. This arrangement of fasteners positively affects the load capacity of the Z-purlins restrained by trapezoidal sheeting in negative position, so it is important for designers to be able to easily determine the values of C_D stiffness in such cases. Therefore, based on the results from the numerical analysis, confirmed by the comparison with the results of experimental studies, a reduction of the value of rotational coefficient C_{100} were proposed in the current provisions of Eurocode 3-1-3 in case of 1+1 fastener arrangement under gravity loading. Also the new value of rotational coefficient C_{100} for cases not covered by the provisions of Eurocode 3-1-3 were presented (1+1 fastener arrangement and the uplift loading, and 2+0 fastener arrangement and both loading cases).

REFERENCES

1. EN 1993-1-3:2006. Eurocode 3 – Design of steel structures - Part 1-3: General rules – Supplementary rules for cold-formed members and sheeting.
2. M. Gajdzicki, J. Goczek: Influence of Sheet-to-purlin Fastener Properties on the Rotational Restraint of Cold-formed Z-purlins. International Journal of Steel Structures 2017, 17(2), pp. 711-721.
3. J. Lindner, T. Gregull: Torsional restraint coefficients of profiled sheeting. In: Proc. of International Association for Bridge and Structural Engineering, Colloquium Stockholm, Zürich, Switzerland, 1986, pp. 161-168.
4. J. Lindner: Restraint of beams by trapezoidally sheeting using different types of connection. In: Usami T, Itoh Y, editors. Stability and ductility of steel structures. Elsevier, 1998, pp. 27-36.
5. T. Vrany: Rotační podepření tenkostěnné ocelové vaznice krytinou. Habilitační práce. Praha, 2002.
6. R.M. Lucas, F.G.A. Al-Bermani, S. Kitipornchai: Modelling of Cold-Formed Purlin-Sheeting Systems. Part 1: Full Model. Thin Walled Structures 1997, 27, pp. 223-243.
7. R.M. Lucas, F.G.A. Al-Bermani, S. Kitipornchai: Modelling of Cold-Formed Purlin-Sheeting Systems. Part 2: Simplified Model. Thin Walled Structures 1997, 27, pp. 263-286.
8. K.B. Katnam, R. Van Impe, G. Lagae, M. De Strycker: A theoretical numerical study of the rotational restraint in cold-formed steel skin purlin-sheeting systems. Computers and Structures 2007, 85, pp. 1185-1193.
9. M. Gajdzicki, J. Goczek: Numerical Determination of Rotational Restraint of Cold-formed Z-purlin According to EC3. International Journal of Steel Structures 2015, 15(3), pp. 633-645.